that within the limits of resolution, a guest AgTPP can have either $S_4$ or the actual site symmetry $C_4$ but does not possess the approximate $C_{4v}$ symmetry or higher. On the other hand, within a slightly larger error, the isotropic hfs for all four pyrrole proton pairs of CuTPP are equal and only one doublet is observed when $H$ is along $g_{\|}$. Thus, there is no evidence of symmetry lower than $C_{4v}$ for CuTPP.

For both AgTPP and CuTPP the proton hfs tensors are anistropic and, furthermore, the observed dipolar contributions are greater for Ag than for Cu and greater than would be calculated from the classical point-dipolar formula. In addition, for the two protons on a given pyrrole ring, the vectors at angles of $\varphi_0$ make a greater angle with the vector along the M–N bond than would be calculated from the crystallographically determined M–H vectors.[11] These features all arise from the distributed nature of the unpaired-electron cloud. They show that the odd electron cannot be considered as a point-dipole located at the metal ion position, and that the extent of the odd-electron delocalization is greater for silver than for copper.

The $^{14}$N hfs tensor is essentially axial with the unique direction along the M–N bond; the slight deviations from axial symmetry again appear to be attributable to the extended nature of the d orbital.[12] These tensor components obtained by ENDOR can be successfully used in computer simulations of the observed EPR spectra (Figure 1). Features of the EPR spectra in an $H_2$TPP host which were previously suggested to indicate nitrogen nonplanarity[1] now appear to arise from a partial resolution of the unequal coupling constants for the two pairs of inversion-related nitrogens.

The $^{14}$N hfs parameters further give information about the relative covalency of the Ag–N bond, involving bonding with a 4d orbital, as opposed to the Cu–N bond. The $^{14}$N isotropic coupling constant, $a^N = (\sum_i A^N{}_i)/3$, is proportional to the nitrogen s-orbital population of the odd electron. As a simplified illustration, if a fixed (sp$^2$) hybridization at N is assumed and polarization effects are ignored, then the ratio $a^N(\mathrm{Ag})/a^N(\mathrm{Cu})$ gives the ratio of the contribution of nitrogen orbitals to the odd-electron wave function. Use of the data in Table I indicates that the contribution is roughly 40% greater in AgTPP and further shows that the d-orbital contribution to the odd-electron wave function for CuTPP is ~65%, while that for AgTPP is only ~50%.[13] This change in covalency with metal atom is in interesting contrast with the rough constancy of nitrogen hyperfine splittings for a number of different copper porphyrins and phthalocyanine.[14] Completion of the complex analysis of the $^{14}$N ENDOR patterns will allow us to obtain the quadrupole coupling parameters, which measure the asymmetry of the total electron distribution around nitrogen; these results will be combined with those presented here in a detailed discussion of the electronic structure of these systems.

**Acknowledgment.** This work has been supported by the National Science Foundation through Grant DMR 7601057 to the Northwestern University Materials Research Center, by National Science Foundation Grant BMS 00478, and by National Institutes of Health Grant HL-13531. We thank Professor J. L. Hoard for the details of the structure of AgTPP.

**Registry No.** AgTPP, 14641-64-6; CuTPP, 14172-91-9; $H_2O$ZnTPP, 16456-79-4.

## References and Notes

(1) For a single crystal EPR study of CuTPP and AgTPP, see P. T. Manoharan and M. T. Rogers, *Electron Spin Reson. Met. Complexes, Proc. Symp., 1968*, 143 (1969).
(2) L. Kevan and L. D. Kispert, "Electron Spin Double Resonance Spectroscopy", Wiley-Interscience, New York, N.Y., 1976.
(3) A. D. Adler, F. R. Longo, F. Kampas, and J. Kim, *J. Inorg. Nucl. Chem.*, **32**, 927 (1969).
(4) B. M. Hoffman, C. J. Weschler, and F. Basolo, *J. Am. Chem. Soc.*, **98**, 5473 (1976).
(5) G. P. Lozos, Ph.D. Dissertation, Northwestern University, 1974.
(6) M. D. Glick, G. H. Cohen, and J. L. Hoard, *J. Am. Chem. Soc.*, **89**, 1996 (1967).
(7) A. Abragam and B. Bleaney, "Electron Paramagnetic Resonance of Transition Ions", Clarendon Press, Oxford, 1970.
(8) V. Ya. Zevin, S. S. Ishchenko, and M. A. Ruban, *Zh. Eksp. Teor. Fiz.*, **55**, 2108 (1968).
(9) After the submission of this paper, an extended discussion of the difficulties created by the nuclear–nuclear coupling has appeared: A. Schweiger, F. Graf, G. Rist, and Hs. H. Günthard, *Chem. Phys.*, **17**, 155 (1976).
(10) Reference 7, Chapter 3.
(11) For a discussion of the AgTPP and CuTPP structures, see J. L. Hoard, *Porphyrins Metallophyrins* (1975).
(12) Note that the $^{14}$N tensors of ref 1 are in error. Their reported $A^N$ and $B^N$ correspond to $A^N{}_3$ and to $(A^N{}_1 + A^N{}_2)/2$, respectively.
(13) For the unit spin-density values, see J. R. Morton, J. R. Rowlands, and D. H. Whiffen, *Natl. Phys. Lab.*, (*U. K.*), *Circ.*, **No. BPR 1.3**.
(14) For a recent compilation, see P. W. Lau and W. C. Lin, *J. Inorg. Nucl. Chem.*, **37**, 2389 (1975).

---

Contribution from the Department of Chemistry,
Tulane University, New Orleans, Louisiana 70118

# Spectroscopic Properties of Vanadium(II), Manganese(II), and Nickel(II) in Crystals of CsCdBr$_3$

Gary L. McPherson* and Kenneth O. Devaney

*Received November 1, 1976* AIC60779V

A considerable number of double salts of the formula $AMX_3$ (where A is a univalent cation, M a divalent metal ion, and X a halide) have been isolated and characterized. When A is a large ion such as cesium or tetramethylammonium, a linear-chain structure similar to that of $CsNiCl_3$ or $(CH_3)_4NMnCl_3$ is usually observed. This structure can be best described as a parallel array of infinite linear chains of $[MX_6]^{4-}$ octahedra-sharing faces. The large cations occupy positions between chains. The spectroscopic and magnetic properties of transition metal salts of this type have been of considerable interest because of the strong one-dimensional character of their structure.

The magnesium salts $CsMgCl_3$, $CsMgBr_3$, and $CsMgI_3$ have been shown to be isostructural with $CsNiCl_3$.[1-3] These diamagnetic materials have proved to be useful host lattices in a variety of spectroscopic and magnetic investigations.[1,2,4-11] Recently it has been found that the cadmium salt $CsCdBr_3$ adopts the $CsNiCl_3$ structure. Thus, $CsCdBr_3$ is also a suitable diamagnetic host material for studying the properties of "isolated" transition metals ions in a linear-chain $AMX_3$ lattice. This paper presents the results of EPR studies of single crystals of $CsCdBr_3$ doped with divalent vanadium, manganese, and nickel. The ligand field spectrum of divalent nickel in $CsCdBr_3$ crystals is also reported. The properties of the paramagnetic ions in $CsCdBr_3$ and $CsMgBr_3$ are carefully compared in order to determine how great an effect a change in host lattice has on an ion's behavior in this series of compounds.

## Experimental Section

**Preparation of Materials.** The salt $CsCdBr_3$ was crystallized by slow evaporation of aqueous HBr solutions containing equimolar amounts of cesium bromide and cadmium acetate dihydrate. The white crystalline solid was dried at 120 °C and stored in stoppered vials. The material is not noticeably hygroscopic. Anal. Calcd for $CsCdBr_3$: Br, 49.36. Found: Br, 49.03.

**Crystal Growth.** Single crystals suitable for spectroscopic and x-ray work were grown from the melt by the Bridgman method. Doped crystals for EPR study were prepared by adding ~0.1% (by weight) of the appropriate transition metal salt to the $CsCdBr_3$. The crystal

Table I. Spin-Hamiltonian Parameters[a]

| | $CsCdBr_3$ | | $CsMgBr_3$[b] | |
|---|---|---|---|---|
| | 297 K | 77 K | 297 K | 77 K |
| V(II) | | | | |
| $g_\parallel$ | 1.993 (3) | 1.994 (3) | 1.996 (2) | 1.996 (2) |
| $g_\perp$ | 1.993 (3) | 1.994 (3) | 1.996 (2) | 1.996 (2) |
| $A$, $cm^{-1}$ | ±0.0072 (2) | ±0.0072 (2) | ±0.0070 (2) | ±0.0070 (2) |
| $B$, $cm^{-1}$ | ±0.0070 (2) | ±0.0070 (2) | ±0.0070 (2) | ±0.0070 (2) |
| $D$, $cm^{-1}$ | ±0.0209 (8) | ±0.0478 (8) | ∓0.132 (2) | ∓0.128 (2) |
| Mn(II) | | | | |
| $g_\parallel$ | 2.004 (3) | 2.004 (3) | 2.004 (1) | 2.004 (1) |
| $g_\perp$ | 2.004 (4) | 2.004 (4) | 2.004 (1) | 2.004 (1) |
| $A$, $cm^{-1}$ | ±0.0076 (2) | ±0.0076 (2) | ±0.0077 (2) | ±0.0077 (2) |
| $B$, $cm^{-1}$ | ±0.0075 (2) | ±0.0075 (2) | ±0.0077 (2) | ±0.0077 (2) |
| $D$, $cm^{-1}$ | ∓0.0373 (8) | ∓0.0340 (8) | ∓0.0950 (10) | ∓0.0930 (10) |
| $\lvert a - F \rvert$, $cm^{-1}$ | 0.0017 (5) | 0.0014 (5) | 0.0013 (2) | 0.0012 (2) |
| Ni(II) | | | | |
| $g_\parallel$ | | 2.22 (1) | | 2.23 (1) |
| $g_\perp$ | | 2.22 (2) | | 2.23 (1) |
| $D$, $cm^{-1}$ | | 1.28 (6) | | 1.70 (2) |

[a] The numbers in parentheses represent the estimated maximum error in the last place of the reported parameter. [b] Taken from ref 9.

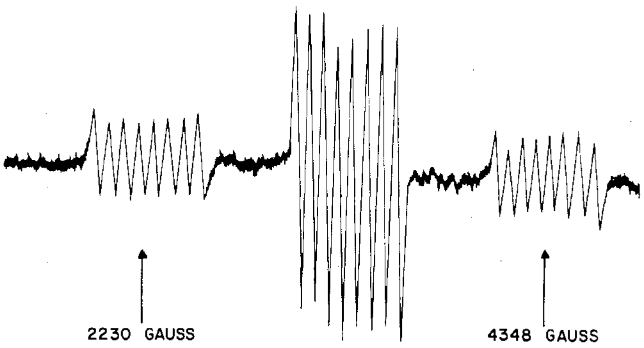

Figure 1. X-Band EPR spectrum of V(II) in $CsCdBr_3$ recorded with the magnetic field parallel to the crystallographic *c* axis.

used for polarized absorption spectroscopy was grown from a sample of $CsCdBr_3$ containing ~0.5% $CsNiBr_3$. The apparatus and procedure have been described previously.[12]

**X-Ray Studies.** A small single crystal of $CsCdBr_3$ was cleaved from a larger crystal grown from the melt. This crystal was mounted on a glass fiber. Precession photographs of the *hk*0, *hhl*, and *hh*+1*l* zones were taken with filtered Mo K$\alpha$ radiation. The material is hexagonal with lattice constants $a = b = 7.66$ Å and $c = 6.70$ Å. The systematic absences (*hhl*; $l \neq 2n$) are consistent with the space groups $P6_3/mmc$, $P6_3mc$, and $P\bar{6}c2$. The pycnometrically determined density agrees very well with that calculated from the lattice constants assuming there are two molecules per unit cell ($\rho_{obsd} = 4.69$ g/cm$^3$; $\rho_{calcd} = 4.73$ g/cm$^3$).

**EPR Spectra.** The tendency of $CsCdBr_3$ to cleave parallel to the crystallographic *c* axis greatly facilitates mounting and orienting the crystals. In most cases the crystals were mounted so that the *c* axis lay in the plane of rotation of the magnetic field. The spectra were recorded at room and liquid nitrogen temperatures on Varian E-3 X-band and E-12 Q-band spectrometers using 100-kHz field modulation. The *g* values were determined by using polycrystalline diphenylpicrylhydrazyl ($g = 2.0036$) as a reference.

**Electronic Spectra.** A crystal of $CsCdBr_3$ doped with Ni(II) was cleaved with a razor blade into a plate having a thickness of 0.44 cm. The crystallographic *c* axis was contained in the plane of the plate. The spectrum of the crystal was studied at room and liquid nitrogen temperatures with the electric vector of the light polarized parallel and perpendicular to the *c* axis. The spectra were recorded from 5000 to 25 000 cm$^{-1}$ on a Cary 14 spectrophotometer. The crystal-mounting procedure and Dewar system have been described previously.[6] Molar extinction coefficients were determined by assuming Beer's law behavior. The nickel content of the sample was determined by chemical analysis. Oscillator strengths were determined by integration of the absorption bands. Because of the many sources of error (baseline, density, analysis, etc.) the oscillator strengths are not expected to have an absolute accuracy better than ±25%; however, the accuracy of the oscillator strengths relative to each other should be considerably better.

## Results and Discussion

**EPR Spectra.** Although a complete structure determination of $CsCdBr_3$ has not been carried out, it seems almost certain that this salt is very similar in structure to the cesium magnesium trihalides. One would expect $CsMgBr_3$ and $CsCdBr_3$ to be identical except for small differences in interatomic distances. (These differences should reflect the larger ionic radius of $Cd^{2+}$ relative to $Mg^{2+}$.) In general, the coordination spheres of the divalent metal ions in the linear-chain $AMX_3$ salts deviate noticeably from regular octahedral geometry. Structural studies on a number of salts have shown that the $[MX_6]^{4-}$ octahedra tend to be elongated along the threefold axis of the $[MX_3^-]_n$ anionic chain (crystallographic *c* axis).[1,13-21] Presumably the electrostatic repulsions between the divalent metal ions cause the $[MX_3^-]_n$ chains to "stretch out". It seems likely that the structure of $CsCdBr_3$ will follow this general trend. In any event, the preliminary x-ray work on $CsCdBr_3$ shows that the cadmium ions must occupy sites which have axial symmetry. As would be expected, the EPR spectra of $CsCdBr_3$ crystals containing divalent vanadium, manganese, and nickel can be accurately described by axial spin Hamiltonians. In all cases the observed resonances can be assigned to a single type of "isolated" ion. Apparently the impurity ions replace the cadmium ions in the $CsCdBr_3$ lattice without causing major structural changes. In contrast with trivalent ions,[22] there appears to be little tendency for divalent ions to cluster in pairs or in higher aggregates when doped into the linear-chain $AMX_3$ lattices.

The interpretation of the spectra and the evaluation of the spin-Hamiltonian parameters of the doped $CsCdBr_3$ crystals are quite straightforward. In general, the same procedures are followed that were used in the analyses of the spectra of V(II), Mn(II), and Ni(II) in the cesium magnesium trihalides.[1,9] The spin Hamiltonians are those which are generally applied to these three ions in axially symmetric environments.[23] The parameters are defined in the same manner as that presented in ref 9. The spectrum of V(II) in $CsCdBr_3$ contains the three-line fine structure expected of a $d^3$ ion in an axial site. The $^{51}V$ nucleus ($I = {}^7/_2$) produces an eight-line hyperfine structure giving a total of 24 lines (see Figure 1). The *g* values, zero-field splitting, and hyperfine parameters (for all three ions) are given in Table I. The relative signs of the

Table II. Assignments, Band Energies, and Oscillator Strengths for the Ligand Field Spectrum of $CsNi_{0.004}Cd_{0.996}Br_3$

| Assignment[a] | Obsd energy, $cm^{-1}$ 298 K | Obsd energy, $cm^{-1}$ 77 K | Calcd energy,[b] $cm^{-1}$ | Polarizn | Oscillator strengths, $f \times 10^5$ 298 K | Oscillator strengths, $f \times 10^5$ 77 K |
|---|---|---|---|---|---|---|
| $^3A_{2g} \rightarrow {}^3T_{2g}$ | 6 200 | 6 500 | 6 500 | $\parallel$ | 5.5 | 1.8 |
| | | | | $\perp$ | 2.9 | 1.2 |
| $^3A_{2g} \rightarrow {}^3T_{1g}(P), {}^1E_g(D)$ | 10 400 | 10 500 | 10 900 | $\parallel$ | 11.6 | 4.6 |
| | 11 200 | 11 600 | | $\perp$ | 8.8 | 4.6 |
| $^3A_{2g} \rightarrow {}^1A_{1g}(G), {}^1T_{2g}(D)$ | 17 000 | 17 000 | | $\parallel$ | 1.0[c] | 0.3 |
| | | | | $\perp$ | 0.7[c] | 0.3 |
| $^3A_{2g} \rightarrow {}^3T_{1g}(P)$ | 19 800 | 20 100 | 20 100 | $\parallel$ | 30.7 | 11.5 |
| | | | | $\perp$ | 27.3 | 11.2 |

[a] The band assignments were made assuming an octahedral ligand field. [b] The energies of the three spin-allowed transitions were calculated assuming $Dq$ and $B$ values of 650 $cm^{-1}$ and 765 $cm^{-1}$, respectively. [c] Only approximate due to extensive band overlap.

zero-field splitting ($D$) and hyperfine parameters ($A$ and $B$) were determined by second-order effects in the hyperfine structure according to the method outlined by Bleaney and Ingram.[24] The spectrum of Mn(II) in $CsCdBr_3$ contains the expected six-line hyperfine structures superimposed on the five-line fine structure. Again the relative signs of the zero-field splitting and hyperfine parameters were determined by the second-order effects in the hyperfine structure. An interesting feature of the Mn(II) spectrum is the appearance of well-resolved ligand hyperfine structure. When the crystals are cooled to 77 K and the field is directed along the $c$ axis ($\theta = 0°$) hyperfine splitting from the bromine nuclei are clearly seen in all five fine-structure components. Unfortunately, a complete analysis of the ligand hyperfine interactions is prevented by the fact that the well-resolved structure appears only when the field is applied parallel to the $c$ axis. The resonances in the spectrum of Ni(II) in $CsCdBr_3$ are only clearly resolved at liquid nitrogen temperature. Because the zero-field splitting is relatively large, the spectrum exhibits a distinctly non-first-order behavior. The analysis of this spectrum required exact solutions to the spin Hamiltonian which were obtained by computer diagonalization of the Hamiltonian matrix.

The spin-Hamiltonian parameters for V(II), Mn(II), and Ni(II) in $CsCdBr_3$ are typical of those generally observed for these particular ions in approximately octahedral environments. The parameters for the same ions in $CsMgBr_3$ are included in Table I for the purpose of comparison. The $g$ values and hyperfine constants are strikingly similar in the two host materials. The zero-field splittings, on the other hand, differ noticeably from $CsCdBr_3$ to $CsMgBr_3$. It appears that the zero-field splitting for V(II) actually changes sign in going from $CsCdBr_3$ to $CsMgBr_3$. (This conclusion assumes that the signs of the $^{51}V$ hyperfine couplings are the same in both lattices). In general, the zero-field splittings in $CsCdBr_3$ seem to be more sensitive to temperature than those in $CsMgBr_3$.

**Ligand Field Spectra.** A study of the ligand field spectrum of Ni(II) in $CsCdBr_3$ was undertaken to determine more precisely how the host lattice affects the properties of these divalent metal ions. Nickel(II) was chosen because its spectrum provides a direct measure of the ligand field splitting energy and thorough studies of the spectra of pure $CsNiBr_3$ and Ni(II) in $CsMgBr_3$ were already available.[2,7] As can be seen from Figure 2 the spectrum of $CsNi_xCd_{1-x}Br_3$ is dominated by the three spin-allowed bands. None of these bands are strongly polarized. The spectrum can be readily assigned on the basis of an octahedral ligand field (see Table II). The calculated (triplet–triplet) transition energies in Table II were obtained from simple crystal field computations using a $Dq$ value of 650 $cm^{-1}$ and an interelectronic repulsion parameter, $B$, of 765 $cm^{-1}$. The band intensities are quite dependent on temperature. The oscillator strengths decrease noticeably when the crystals are cooled from room to liquid nitrogen temperature (see Table II). This decrease is characteristic of a vibronic intensity mechanism and would be expected for the d–d transitions of an octahedral transition metal complex. In terms of the three spin-allowed bands, the spectra of pure $CsNiBr_3$, $CsNi_xMg_{1-x}Br_3$, and $CsNi_xCd_{1-x}Br_3$ are very similar. The intensities and transition energies are essentially the same in all three spectra. Crystal field calculations for the spectra of $CsNi_xMg_{1-x}Br_3$ and $CsNiBr_3$ give $Dq$ and $B$ values of 655 and 766 $cm^{-1}$, respectively.[2] The spectrum of pure $CsNiBr_3$ differs from those of $CsNi_xMg_{1-x}Br_3$ and $CsNi_xCd_{1-x}Br_3$ in only one important respect. It contains a number of fairly intense absorptions which are not present (or only weakly present) in the spectra of the other two materials. These absorptions have been assigned to spin-forbidden triplet–singlet transitions which have been made allowed by the magnetic exchange interactions present in pure $CsNiBr_3$.[2,7]

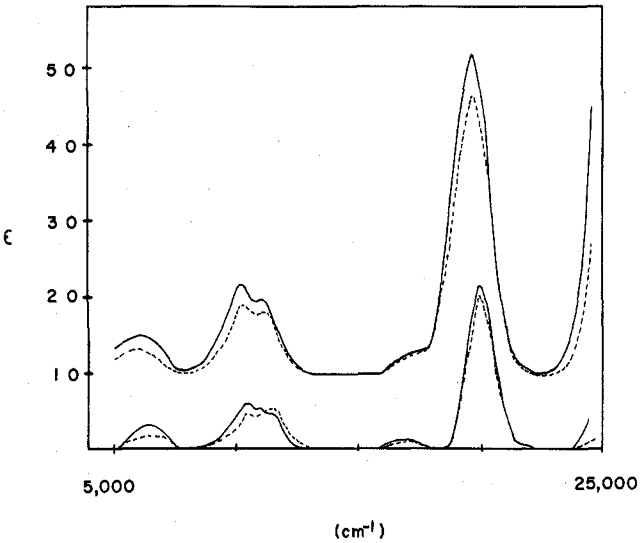

Figure 2. Ligand field spectrum of $CsNi_{0.004}Cd_{0.996}Br_3$. The upper trace corresponds to the room-temperature spectrum while the lower trace shows the liquid nitrogen temperature spectrum. The upper trace is displaced upward by 10 units. The solid lines represent the spectrum recorded with the electric vector of the light polarized parallel to the crystallographic $c$ axis. The dotted lines show the perpendicular polarization.

## Conclusions

It seems virtually certain that the volume occupied by a cadmium ion in $CsCdBr_3$ is larger than that taken up by a magnesium ion in $CsMgBr_3$. A comparison of the lattice constants for the two salts supports this conclusion (for $CsCdBr_3$, $a = 7.66$ Å, $c = 6.70$ Å; for $CsMgBr_3$, $a = 7.60$ Å, $c = 6.50$ Å[2]). Thus, one might expect that a divalent impurity in a $CsCdBr_3$ crystal would occupy a somewhat larger site than in a $CsMgBr_3$ crystal. The fact that the $g$ values and hyperfine constants for each ion are so similar in the two host lattices seems to suggest that this is not really the case. The $^{51}V$ and

$^{55}$Mn hyperfine coupling constants indicate that the extents of metal to ligand delocalization are approximately the same in the two host materials, for both V(II) and Mn(II). According to simple crystal field theory the *g* values of octahedral complexes containing d$^3$ or d$^8$ ions can be described by $g = 2 - 8\lambda/10Dq$.[25] Assuming that this expression is at least qualitatively correct, one would conclude that the ligand field splittings (10*Dq*) for Ni(II) and V(II) do not change significantly in going from $CsMgBr_3$ to $CsCdBr_3$. This conclusion is certainly supported by the similarity of the ligand field spectra of $CsNi_xMg_{1-x}Br_3$ and $CsNi_xCd_{1-x}Br_3$. It appears that the average distances between the impurity ion (V(II), Mn(II), or Ni(II)) and the six surrounding bromide ions are approximately the same in both host materials. Apparently the bromide ions in $CsMgBr_3$ and $CsCdBr_3$ are able to adjust their positions to match the size of a divalent impurity which is incorporated into the $[MBr_3^-]$ chains. One might describe these linear-chain salts as "accommodating" host lattices. This type of behavior is not generally typical of ionic host lattices. For example, it is quite evident from studies of V(II) crystals of $CsCdCl_3$[26] and $CsCaCl_3$[27] that the average metal–chlorine distances for the impurity ion are determined primarily by the host lattice. (Neither of these two host materials adopt the linear-chain $CsNiCl_3$ structure.)

It should be remembered that unlike the *g* values and hyperfine constants, the zero-field splittings of the three ions do differ significantly between $CsCdBr_3$ and $CsMgBr_3$. The zero-field splitting presumably reflects the trigonal distortion of a paramagnetic ion's environment. Thus, while the average metal–bromine distances for the three transition metal ions do not appear to change much from $CsCdBr_3$ to $CsMgBr_3$, the actual geometry of the $[MBr_6]^{4-}$ complex must vary significantly from one host material to the other.

**Registry No.** V(II), 15121-26-3; Mn(II), 16397-91-4; Ni(II), 14701-22-5; $CsCdBr_3$, 16593-55-8.

## References and Notes

(1) G. L. McPherson, T. J. Kistenmacher, and G. D. Stucky, *J. Chem. Phys.*, **52**, 815 (1970).
(2) G. L. McPherson and G. D. Stucky, *J. Chem. Phys.*, **57**, 3780 (1972).
(3) T. Li, G. D. Stucky, and G. L. McPherson, *Acta Crystallogr., Sect. B*, **29**, 1330 (1973).
(4) N. Achiwa, *J. Phys. Soc. Jpn.*, **27**, 561 (1969).
(5) H. Rinneberg and H. Hartmann, *J. Chem. Phys.*, **52**, 5814 (1970).
(6) G. L. McPherson, T. J. Kistenmacher, J. B. Folkers, and G. D. Stucky, *J. Chem. Phys.*, **57**, 3771 (1972).
(7) J. Ackerman, E. M. Holt, and S. L. Holt, *J. Solid State Chem.*, **9**, 279 (1974).
(8) G. L. McPherson, H. S. Aldrich, and J. R. Chang, *J. Chem. Phys.*, **60**, 534 (1974).
(9) G. L. McPherson, R. C. Koch, and G. D. Stucky, *J. Chem. Phys.*, **60**, 1424 (1974).
(10) S. L. Holt, *ACS Symp. Ser.*, **5**, 164 (1975).
(11) C. F. Putnik, G. M. Cole, Jr., B. B. Garnett, and S. L. Holt, *Inorg. Chem.*, **15**, 826 (1976).
(12) G. L. McPherson, L. J. Sindel, H. F. Quarls, C. B. Frederick, and C. J. Doumit, *Inorg. Chem.*, **14**, 1831 (1975).
(13) G. D. Stucky, S. D'Agostino, and G. L. McPherson, *J. Am. Chem. Soc.*, **88**, 4828 (1966).
(14) B. Morosin and E. J. Graeber, *Acta Crystallogr.*, **23**, 766 (1967).
(15) A. Engberg and H. Soling, *Acta Chem. Scand.*, **21**, 168 (1967).
(16) H. Soling, *Acta Chem. Scand.*, **22**, 2793 (1968).
(17) G. D. Stucky, *Acta Crystallogr., Sect. B*, **24**, 330 (1968).
(18) R. W. Asmussen, T. K. Larsen, and H. Soling, *Acta Chem. Scand.*, **23**, 2055 (1969).
(19) D. Babel, *Z. Anorg. Allg. Chem.*, **369**, 117 (1969).
(20) B. Morosin, *Acta Crystallogr., Sect. B*, **28**, 2303 (1972).
(21) J. Goodyear and D. J. Kennedy, *Acta Crystallogr., Sect. B*, **28**, 1640 (1972).
(22) G. L. McPherson and W. Heung, *Solid State Commun.*, **19**, 53 (1976).
(23) A. Abragam and B. Bleaney, "Electron Paramagnetic Resonance of Transition Metal Ions", Clarendon Press, Oxford, 1970, Chapter 7.
(24) B. Bleaney and D. J. E. Ingram, *Proc. R. Soc. London, Ser. A*, **205**, 336 (1951).
(25) C. J. Ballhausen, "Introduction to Ligand Field Theory", McGraw-Hill, New York, N.Y., 1962, Chapter 10.
(26) J. R. Chang, G. L. McPherson, and J. L. Atwood, *Inorg. Chem.*, **14**, 3079 (1975).
(27) G. L. McPherson and M. R. Freedman, *Inorg. Chem.*, **15**, 2299 (1976).

---

Contribution from the Chemistry Department,
University of Tasmania, Hobart, Tasmania, Australia 7001

# Molecular *g* Values of the Planar $CuCl_4^{2-}$ Ion

P. Cassidy and M. A. Hitchman*

*Received November 9, 1976* AIC60817A

Because of the comparative simplicity of its electronic structure considerable theoretical interest has been shown in planar $CuCl_4^{2-}$, and several molecular orbital (MO) calculations[1-3] have been carried out on this ion. It has also been used as a model in the calculation of the EPR parameters[4,5] and electronic spectral transition energies[6] of metal complexes. The various MO calculations have suggested the orbital energy sequences $b_{1g}(d_{x^2-y^2}) >> a_{1g}(d_{z^2}) > e_g(d_{xz}, d_{yz}) > b_{2g}(d_{xy})$[2,3] and $b_{1g}(d_{x^2-y^2}) >> b_{2g}(d_{xy}) > e_g(d_{xz}, d_{yz}) > a_{1g}(d_{z^2})$,[1] while the orbital scheme $b_{1g}(d_{x^2-y^2}) >> b_{2g}(d_{xy}) > a_{1g}(d_{z^2}) > e_g(d_{xz}, d_{yz})$ has also been proposed[7] in a general MO treatment of planar metal complexes (the symmetry labels refer to the $D_{4h}$ point group with the *x* and *y* axes lying along the bond directions). The further suggestion has been made that, despite an orbital sequence placing $d_{z^2}$, $d_{xz}$, $d_{yz}$, and $d_{xy}$ all comparatively close in energy, interelectron repulsion effects will give rise to a sequence of *state* energies $^2B_{2g}(d_{xy}) \sim {}^2A_{1g} >> {}^2E_g >> {}^2B_{1g}$. It is only recently that a compound containing a strictly planar $CuCl_4^{2-}$ ion has been prepared:[8] $(N\text{-mph})_2CuCl_4$ (*N*-mph = *N*-methylphenethylammonium). Other complexes of general type $[\text{cation}]_2CuCl_4$ of known structure contain either distorted tetrahedral anions or polymeric structures with long axial bonds joining planar $CuCl_4^{2-}$ groupings.[9] In order to elucidate the electronic properties of isolated planar $CuCl_4^{2-}$ we have studied the single-crystal electronic and EPR spectra of $(N\text{-mph})_2CuCl_4$. The low-temperature "d–d" polarized electronic spectrum of the complex shows three well-resolved peaks at 11 760, 13 700, and 16 100 cm$^{-1}$, with each peak showing remarkably well-resolved vibrational fine structure.[10] Initial measurements made on the (010) crystal face pointed tentatively to the state energy sequence $^2E_g > {}^2B_{2g} > {}^2A_{1g} >> {}^2B_{1g}$.[10] Subsequent measurements on other crystal faces, however, now suggest[11] rather strongly the sequence $^2A_{1g} > {}^2E_g > {}^2B_{2g} >> {}^2B_{1g}$.

To complement the electronic spectral data we have measured the EPR spectra of single crystals of $(N\text{-mph})_2CuCl_4$ at room temperature using a JEOL JES-P-10 EPR spectrometer operating at X-band frequency for rotations of the magnetic field in the (010), (001), and *bc** crystal planes. A sample of 1% $Mn^{2+}$ in MgO was used to calibrate the spectra and the values of $g^2$ for various orientations of the magnetic field are listed in Table I. Treatment of the data by a method described previously[12] yields the molecular *g* values $g_x = 2.040$ (0.002), $g_y = 2.040$ (0.004), and $g_z = 2.221$ (0.004), where the figure in parentheses represents the possible error. Here *x* and *y* were defined along the shorter and longer Cu–Cl bond directions (224.8 and 228.1 pm[8]), respectively. Within experimental error, the **g** tensor thus has axial symmetry. The molecular *g* values of planar $CuCl_4^{2-}$ have been calculated by Smith[4] using expressions which include charge-transfer states and the ligand portion of the ground-state wave function. These expressions are of the form

$$\Delta g_{\parallel} = K_{\parallel}(\text{d-d})/E[B_{2g}(\text{d-d})] + K_{\parallel}(\text{ct})/E[B_{2g}(\text{ct})] \qquad (1)$$

$$\Delta g_{\perp} = K_{\perp}(\text{d-d})/E[E_g(\text{d-d})] + K_{\perp}(\text{ct})/E[E_g(\text{ct})] \qquad (2)$$

where $\Delta g_{\parallel}$ and $\Delta g_{\perp}$ represent the *g* shifts relative to the free-electron value parallel and perpendicular to the symmetry axis, $E[B_{2g}(\text{d–d})]$ etc. represent the energies of the appropriate excited d–d or charge transfer (ct) states, and the values of $K_{\parallel}$ and $K_{\perp}$ depend on the spin–orbit coupling constants of